# Complex role for thallium in PbTe:Tl from local probe studies

T. Keiber, F. Bridges, B.C. Sales, and H. Wang

Phys. Rev. B **87**, 144104 — Published 22 April 2013

DOI: 10.1103/PhysRevB.87.144104

# The Complex Role for Thallium in PbTe:Tl from Local Probe Studies

T. Keiber,[1] F. Bridges,[1] B. C. Sales,[2] and H. Wang[2]

[1] *Physics Department, University of California, Santa Cruz, California 95064, USA*
[2] *,Materials Science and Technology Division, Oak Ridge National Laboratory, Oak Ridge, Tennessee 37831, USA*

When PbTe, a good thermoelectric material, is doped with a few percent Tl, the figure of merit, $ZT$=$TS^2/(\rho\kappa)$ [$S$ is the Seebeck coefficient, $\rho$ the electrical resistivity, and $\kappa$ the thermal conductivity], is dramatically improved. The maximum value of $ZT$ occurs for approximately 2% Tl but the factors limiting $ZT$ are as yet, poorly understood. From a detailed local structure study of PbTe:Tl using the Extended X-ray Absorption Fine Structure (EXAFS) technique, we find that Tl substitutes primarily as Tl(+1) on the Pb site, with no evidence for any solubility issue, any significant fraction of Tl(+3), or any Tl interstitials. However it is not a simple substitution as there is evidence for increasing Te vacancies on neighboring sites with increasing Tl concentration, x. In addition there is also increasing disorder with x – Tl-Te bond length disorder as well as the vacancy defects – that will scatter the hole carriers and begin to increase the electrical resistivity in spite of an increase in hole concentration. This increased disorder is likely an important factor limiting $ZT$.

## I. INTRODUCTION

For several decades there have been intensive studies of thermoelectric materials, to better understand and eventually control those properties that are important for thermoelectric applications.[1–3] The figure of merit, $ZT$ = $TS^2/(\rho\kappa)$, is a convenient parameter for characterizing the quality of such materials. In most cases, good thermoelectrics are semiconductors with relatively high Seebeck coefficients and quite low electrical resistivity, with the thermal conductivity determined primarily by the lattice phonons. One example is PbTe. The pure compound is already a good thermoelectric, but when doped with a small amount of Tl ($Pb_{1-x}Tl_xTe$), $ZT$ improves significantly to $\sim$ 1.5 near 800K for 2% Tl; much of this increase is attributed to an enhancement in $S$ at high hole concentrations for the Tl doped samples, as a result of a change of the density of states near the top of the valence band.[4,5] At much lower Tl concentrations ($\sim$ 0.2% Tl) $S$ is larger[6] but the electrical resistivity is much higher. Unfortunately for x > 2%, $ZT$ again decreases. It is important to understand the factors limiting $ZT$ for such materials, since doping is a promising approach to greatly improve $|S|$ and hence $ZT$. Similar but smaller improvements in $ZT$ have also found in Na doped PbTe.[7]

To date, little is known about the local structure about the Tl atom or how Tl enters the PbTe lattice, although local structure studies of pure PbTe (PDF analysis) exist.[8,9] Tl doping produces p-type PbTe but the hole concentration increases more slowly than the Tl concentration. This could arise in a number of ways: there might be a solubility limit for Tl as suggested by Singh,[10] or there may be charge compensation - from a mixture of Tl(+1) and Tl(+3) sites, interstitial Tl which will have short Tl-Pb/Te bonds, or an increase in Te vacancies.

An important aspect of Tl (and some other) doping for high $ZT$ is a significant increase in $|S|$ related to an increase in the hole density of states (DOS) near the Fermi surface, possibly from a resonance enhancement.[4,10] However there is little discussion about conductivity. Here we examine the local structure about Tl for 1, 2 and 3% concentrations to investigate solubility issues such as the formation of nano-precipitates, various charge compensation mechanisms and the extent of disorder about Tl, which is important for understanding electrical transport. A knowledge of such local structure is crucial for modeling the behavior of such doped thermoelectrics; a preliminary study of the 1% sample has been reported.[11]

## II. EXPERIMENTAL DETAILS

Tl doped $Pb_{1-x}Tl_xTe$ samples, with nominal values of x = 0.01, 0.02, 0.03 were prepared by first melting the elements ( > 99.99% purity) in an evacuated carbon-coated silica tube at 1300 K for 24 h with occasional stirring; the furnace was then cooled to 800 K and the sample annealed for one week. The material was lightly ground by hand into a fine powder in an argon glove box, loaded into a 1.9 cm diameter graphite die and hot-pressed in vacuum at 790 K for 1 hour. X-ray diffraction indicated only the rock salt PbTe phase for the 1 and 2% Tl doped sample; the 3% sample is similar with possibly a tiny ($\leq$ 0.8 wt %) impurity fraction of $Tl_4PbTe_3$. See Ref. 12 for further details.

The dense polycrystalline samples were cut into rectangular bars ($\sim$ 1.5 x 1.5 x 12 $mm^3$) for electrical and Seebeck measurements, and into 1.5 mm thick disks for thermal diffusivity measurements. Rectangular plates approximately 8 x 5 x 0.4 $mm^3$ were cut for the Hall measurements. Electrical contacts to the crystals were made with Ag epoxy or Ag paste (below room temperature) or with spring-loaded gold contacts (above room temperature). Low temperature measurements were made with the thermal transport option (TTO) from Quantum Design in a Physical Property Measurement System (PPMS). High temperature electrical and Seebeck measurements were made in an ULVAC ZEM-3, and thermal diffusivity measured in an Antler FL-5000. The thermal conductivity was calculated using the measured heat capacity of PbTe.[13] See Refs. 14 and 15 for additional de-

tails.

For the XAS experiments polycrystalline material was ground, passed through a 400 mesh sieve, and brushed onto tape, forming a uniform thin layer of small particles. Two layers of tape were pressed together to encapsulate the fine powder. This double layer was then cut into small strips ($\sim 3 \times 18$ mm) and five layers were stacked to provide an absorption edge step of $\sim 0.5$ at the Pb $L_{III}$ edge. For the pure PbTe XAS sample a small piece of single crystal used previously,[12] was ground and prepared in a similar manner. (see Ref. 16 for further XAS details).

The XAS experiments were carried out at the Stanford Synchrotron Radiation Lightsource (SSRL) on beamline 4-1 using Si 220 monochromator crystals. Data were collected in fluorescence mode for the Tl $L_{III}$-edge, with the sample at 45° to the incident X-ray beam. The Pb $L_{III}$ edge data for PbTe and the Tl $L_{III}$-edge data for a TlTe reference sample were collected in transmission. The energy resolutions were $\sim 1.2$ eV for the 1 and 3% samples and 1.4 eV for the 2% sample. To minimize harmonics, the monochromator was detuned 50% for all edges. For each edge/temperature, three scans were collected to check reproducibility and to estimate relative errors.

The EXAFS data were reduced using the RSXAP package.[17] Most of the reduction followed standard procedures,[16,17] but for the low concentration Tl $L_{III}$-edge, an exponentially rising background was observed in the fluorescence detector. It arises from the weak Pb X-ray Raman line of the host which can interfere with the weak Tl fluorescence from the low concentration dopant. Such interference can exist when dilute dopants of atomic number Z are in a host containing atom with atomic number (Z+1) - here Pb. Below the Pb $L_{III}$ edge, the Pb (Z+1) Raman line, is at a fixed energy below the incident energy. As the X-ray energy is swept for the Tl $L_{III}$ data, the Raman line passes through the fluorescence window set up for Tl and its intensity grows as the x-ray energy increases. We have developed a means to correct for this situation[18] and apply it here to the Tl data. Also note that because the Tl edge is only 377 eV below the Pb $L_{III}$ edge, the $k$-space range for the Tl $L_{III}$ data is limited to less than 9 Å$^{-1}$. For comparison purposes we use the same Fourier Transform (FT) range for all data, although the Pb $L_{III}$ data for PbTe (and also the Tl $L_{III}$ data for TlTe - not shown) have good k-space data out to $\sim 15$ Å$^{-1}$ as shown in Fig. 1.

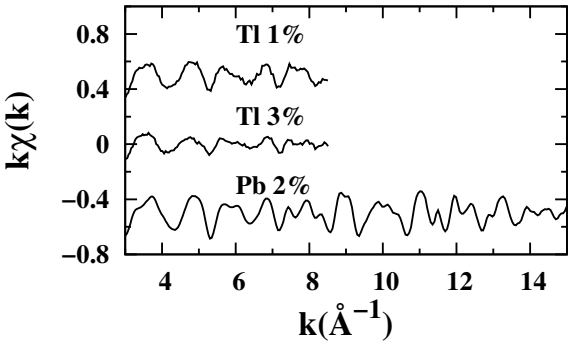


FIG. 1. Examples of the k-space data at the Tl $L_{III}$ edge for 1 and 3% Tl samples and the corresponding Pb $L_{III}$ edge data at the bottom which extends to 15 Å$^{-1}$. The Tl edge data are limited by the presence of the Pb $L_{III}$ edge. Note that the shape of the Tl k-space data is similar to that for the Pb data but broadened.

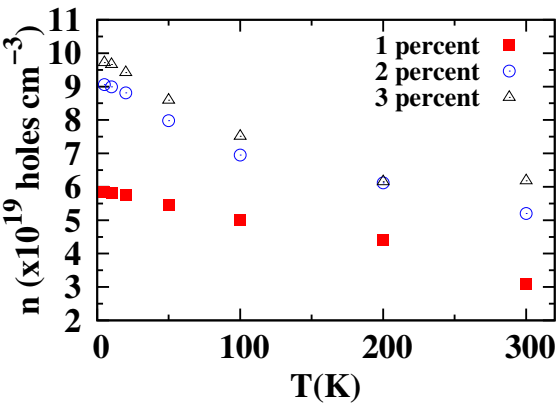


FIG. 2. Hole concentration as a function of $T$ for PbTe:Tl samples doped with 1, 2, and 3 % Tl. Note that the hole concentration increases much slower than the nominal concentration, and the increase between 2 and 3 % Tl is quite small. Part of this decreased hole concentration for the higher dopant concentrations, is likely a result of charge compensation.

## III. TRANSPORT PROPERTIES

In Fig. 2 we plot the measured Hall coefficient as a function of T for the 1-3 % Tl samples. The number of holes does increase with doping but much slower than the increase in nominal doping. To check the concentration of Tl in the doped sample we used the step height ratio at the $L_{III}$ edges of Tl and Pb, at the same point on the XAS sample. The measured concentrations were close to the nominal values: 1 % (0.88 %); 2 % (1.61 %); 3% (3.06 %). Thus within this concentration range, Tl is going into the sample, in agreement with Rustamov *et al.*[19] who reported a solubility $> 5$ %. However transport measurements or x-ray absorption edge steps are not sensitive as to how Tl enters the sample; i.e are there nano-precipitates present or is charge compensation occurring?

Although the hole concentration is increasing, the resistivity, $\rho$, also increases with Tl concentration at low $T$ - see Fig. 3, and at high T, $\rho$ is lowest for the 2% sample. The decreased mobility can arise from an increase in the effective mass with x as a result of non-parabolic valence bands, and/or from increased scattering from defects around Tl.

The Seebeck coefficient (Inset Fig. 4) decreases slightly

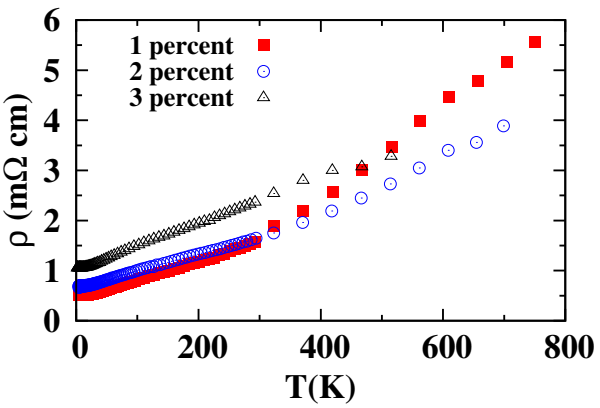


FIG. 3. Resistivity, $\rho$, for 1, 2, and 3 % PbTe:Tl samples. Although the hole concentration increases slowly with dopant concentration, the resistivity also increases; the decreased mobility suggests either increased scattering or an increase in effective mass (or both).

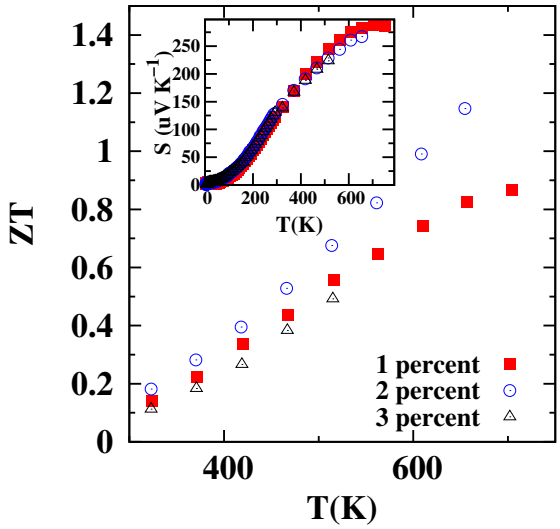


FIG. 4. The figure of merit, $ZT$, for the 1, 2, and 3 % Tl samples. $ZT$ is largest for the 2% sample as found previously. Inset: $S$ vs $T$ showing that $S$ changes $< 10\%$ between samples.

with increasing Tl concentration but changes less than 10 % between our samples. These values of S are also similar to other published works.[4,19] Since the thermal conductivity, $\kappa$, above room temperature changes little with Tl doping[4] the dominant factor determining the figure of merit, $ZT$, is the electrical resistivity. As shown in Fig. 4, $ZT$ is maximum for the 2% sample, and the value for the 3 % sample is lower than for the other two samples. Thus these data raise two important issues: how does increasing Tl concentration increase the carrier concentration and what effects may be limiting the carrier concentration as the dopant concentration increases?

## IV. EXAFS RESULTS

In Fig. 5, we plot the (Fourier Transformed) r-space Tl $L_{III}$ data at low $T$ for each concentration, as well as the Pb $L_{III}$ edge data, and the Tl $L_{III}$ edge data of a TlTe reference sample; a simulation for $Tl_4PbTe_3$ using FEFF[20] is also included.

For the PbTe:Tl data, the first peak at approximately 2.9 Å is from the Tl-Te pair; the second peak (5.0 Å) is composed of a mixture of the first Tl-Pb peak and the second Tl-Te contributions, while the peak near 6.8 Å is the sum of several single scattering and multi-scattering paths. The Tl $L_{III}$ edge data from a TlTe reference sample (bottom plot) is quite different from the plots for the PbTe:Tl sample - the main peak occurs at a longer distance indicating longer Tl-Te bonds in TlTe. For $Tl_4PbTe_3$, the difference is even larger - the peaks are at different positions and a dip occurs where the first main peak in PbTe:Tl is observed.

The Tl $L_{III}$ data exhibit several unusual aspects. First, the shapes of the three main peaks in the Tl data are very similar to that in the Pb data, and the amplitudes of the second and third peaks change little with increasing x. Second, the zero-crossings for the real part of the FT are identical for the peaks near 5 and 6.8 Å, for all scans. Shifts of the zero-crossings correspond to changes in pair-distances $r$; the tiny variation in the zero-crossings between 4.5 and 7 Å places an upper limit of 0.02-0.03Å for any changes in $r$. These two results mean that the more distant environment about Tl is the same in every PbTe:Tl sample and very similar to that of Pb. Which means that Tl substitutes on the Pb site, since there are the same types of neighbors and nearly identical pair distances. The reduced amplitude means increased disorder but it is very unusual that the change in disorder with increasing x is larger for the first peak compared to the further neighbors. Typically if there is significant disorder for the first peak the more distant peaks have an even larger broadening.

There are several explanations for a decreased amplitude. First, increased disorder about a dopant atom is generally expected. If solubility were an issue, other phases might be present including an amorphous phase, but usually is such cases the entire EXAFS plot has a decreasing amplitude as the dopant concentration increases and the phase of the real part of the FT, $R$, shifts; that is not observed here. Finally, when a +1 dopant replaces a +2 host atom, some charge compensation is expected, such as Te vacancies (one vacancy for every two Tl atoms), some Tl in an interstitial site, or some Tl(+3). Note that neighboring Te vacancies would decrease the Tl-Te peak amplitude but may have little effect on further neighbors. To address these issues we have carried out detailed fits of the data to a sum of theoretical (FEFF) functions[20] for the first few shells; here we focus primarily on the nearest neighbor Tl-Te shell. In a few fits we have considered the possibilities of a small fraction of TlTe or $Tl_4PbTe_3$ present, or a small fraction

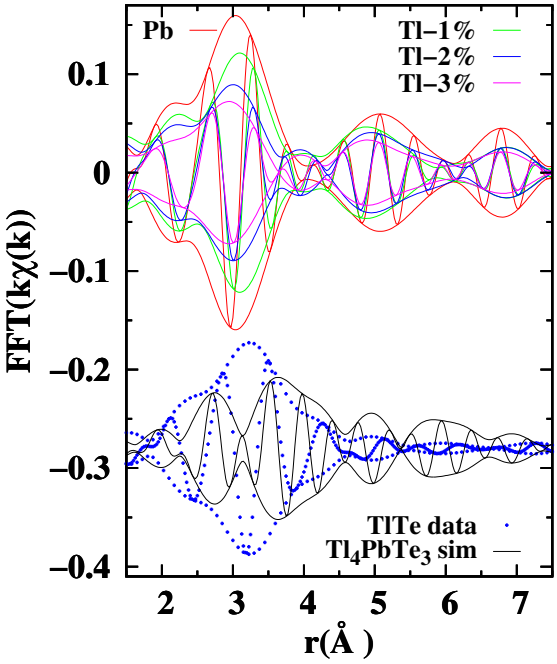


FIG. 5. (Top) $r$-space (FT) EXAFS data at the Tl $L_{III}$ edge for 1 to 3 % Tl concentrations (1% at 10 K; 2 and 3% at 5 K), and the Pb $L_{III}$ edge from the pure PbTe sample; FT range 3.3 to 8.2 Å$^{-1}$ with a Gaussian rounding of 0.2 Å$^{-1}$. (Bottom) The corresponding Tl $L_{III}$ data for pure TlTe and a FEFF simulation for $Tl_4PbTe_3$ are plotted for comparison. In $r$-space data, the fast oscillating function is the real part, $R$, of the FT while the envelop functions are $\pm\sqrt{R^2+I^2}$ with $I$ the imaginary part of the FT.

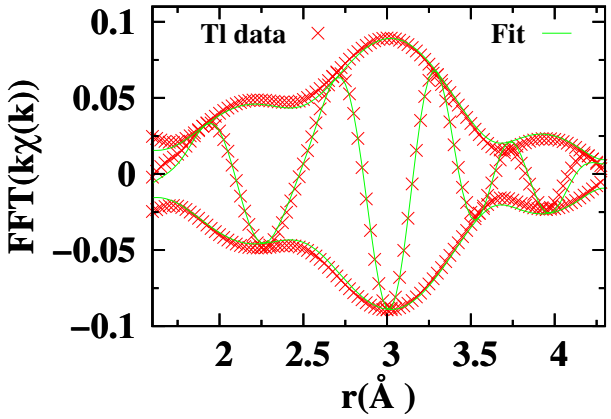


FIG. 6. Tl $L_{III}$ edge $r$-space data for 2% Tl in PbTe plus the fit of the data (solid line) over the region 1.7-4.3Å; same FT range as in Fig. 5. First peak parameters: N = 5.2; $\sigma^2$ = 0.0084 Å$^2$; $r$ = 3.268 Å.

of interstitial Tl sites.

Fits were carried out in $r$-space; for the Tl-Te peak we varied the amplitude, $NS_o^2$ (N – coordination number; $S_o^2$ – amplitude reduction factor from multi-scattering effects), the pair distribution width, $\sigma$, and the bond length $r$. For the corresponding Pb $L_{III}$ edge data, $S_o^2$ is $\sim 0.9$ and we expect it to be similar for Tl as it is a neighbor to Pb in the periodic table. An example of a fit for the 2% sample is shown in Fig. 6; first peak parameters are given in caption. There are strong correlations between N and $\sigma$ when they are both varied and the values of N can vary $\sim$ 12% for a given scan. Nevertheless the fits always show a decrease in N with increasing x for every sample, for each scan, and for all the low temperature data. N is close to 6 (5.7) for the 1 % sample, but is roughly 5 for the 3 % Tl sample - see Table I. For the 2 and 3% samples, reducing N gives a much better fit than holding N constant and modeling the reduced amplitude with $\sigma$ alone. In addition, the Tl-Te bond length is longer than the Pb-Te bond length by $\sim$ 0.04 Å, consistent with Tl(+1) being larger than Pb(+2).

Fits with various quantities of TlTe included (using the 10K TlTe data as an experimental standard), did not improve the fits as judged by Hamilton's F-test;[21] also the amplitude of the TlTe component shifted towards zero. Similarly, assuming a small fraction of Tl interstitial which adds a peak with a short bond length and a complex peak between 2.5 and 3 Å, or some $Tl_4PbTe_3$ did not improve the fits. We cannot say there are no precipitates or Tl interstitials, but if present, they are at most a few percent of the Tl. Split-peak fits of the Tl-Te shell (as suggested for Pb-Te[9]) were precluded because of the short FT range (3.3-8.2 Å$^{-1}$) for the Tl data.

From fits to several traces at low T for the Tl $L_{III}$ edge data, we obtained an average value of $NS_o^2$ for each sample (Tl-Te pair), and then fixed the amplitude at this average value for further fits (as a function of temperature) to extract $\sigma$(T). From these results and fits of TlTe, the value of $S_o^2$ is consistent with that for Pb, $\sim$ 0.9. In Fig. 7 we plot $\sigma^2(T)$ of the the Tl-Te pair for the three Tl concentrations, as well as the results for the Pb-Te pair for comparison using the same short FT range. Above 200K the amplitude of the Tl data is small and the signal to noise becomes too low to obtain good fits. There is a systematic vertical increase in $\sigma^2$(T) as the Tl concentration increases, but to first order the $\sigma^2$(T) plots have similar slopes for the three Tl and the Pb samples. We have fit $\sigma^2$(T) to a correlated Debye model which treats the unit cell as a simple unit cell. The correlated Debye temperatures, $\theta_{cD}$, and static off-sets, $\sigma^2_{static}$, are tabulated in the figure caption. The values of $\theta_{cD}$ are nearly the same for all samples indicating similar effective spring constants between Tl and Te (and between Pb and Te). These relatively low Debye temperatures are similar to those found in other thermoelectric materials such as the skutterudites.[16,22] Note that the static values, $\sigma^2_{static}$, depend on the value of N used; to first order an increase in N shifts the $\sigma^2$(T) plot vertically. Although it is difficult to separate changes in N from increases in $\sigma^2_{static}$, the data consistently indicate that as the Tl concentration increases there is both an increase in the static distortion about Tl and a decrease in the number of nearest

TABLE I. Properties for the Tl local structure in PbTe:Tl including: the measured concentration of Tl by XANES, the correlated Debye temperature for the Tl-Te pair, the corresponding static offset, and the calculated nearest neighbor Te shell coordination number. The error in N is for a single scan but the same results are obtained for 6-9 traces at low T. The values for the Pb-Te pair are shown on the last line for comparison.

| Doping | Conc. | $\theta_{cD}$ (K) | $\sigma^2_{static}$ (Å$^2$) | N |
|---|---|---|---|---|
| Tl 1% | 0.88% | 114 | 0.0031 | 5.7(0.7) |
| Tl 2% | 1.61% | 109 | 0.0060 | 5.1(0.7) |
| Tl 3% | 3.06% | 115 | 0.0083 | 4.6(0.7) |
| Pb-Te | - | 120 | 0.0007 | 6.0 |

neighbor Te atoms. In Table I the error in N is for a single scan; the averaged error for 6-9 traces is considerably smaller (more than a factor of 2), but because of the correlations, statistical averaging is questionable and we only give the error for a single scan.

## V. DISCUSSION AND CONCLUSIONS

In summary, Tl dopants play a complex role in determining the unusual thermoelectric properties of PbTe:Tl. From the ratio of the Tl and Pb step heights, the Tl concentrations are close to the nominal values. In addition, the identical phase of the real part of the FT for the Tl and the Pb $L_{III}$ edge data, from 4.5 to 7 Å, - see Fig. 5 means that the types of neighbors about Tl and the distances to them are identical to the further environment about Pb. Thus, we conclude that Tl substitutes on the Pb site, with no evidence for solubility issues or the presence of interstitials. This precludes the possibility that a significant fraction of the Tl has formed a precipitate of another structure; however one cannot exclude that a small fraction, perhaps $\sim 5\%$ of the Tl, might be in such a phase. There is also the possibility that the presence of Tl and an associated Te vacancy might lead to the formation of smaller PbTe:Tl grain sizes - but these should not be considered precipitates.

Earlier studies[23] indicated that Tl has a single valence in PbTe and our recent XANES[11] also showed no evidence for two valence states. The current results show that the environment about Tl is slightly expanded (0.03-0.04 Å) as expected for a large Tl(+1) defect. Thus all experiments are consistent with a primarily Tl(+1) defect.

However, doping with Tl is not a simple substitution on the Pb site. The significant decrease in amplitude for the Tl-Te peak with increasing x (Fig. 5), with little change in the amplitudes of the further neighbor peaks, indicates that nearest neighbor Te vacancies are present which will compensate the Tl(+1) dopant. The small increase in hole doping with increasing x, particularly from 2-3% Tl, is consistent with significant charge compensation.

The third important aspect of Tl doping is an increase in the local disorder about the Tl site - both from increasing disorder in the Tl-Te bondlength distribution and the increase in Te vacancies - as x increases. In contrast the thermally induced contributions to the disorder for the Tl-Te pair are the same for all values of x; the values of $\theta_{cD}$ are similar for all the Tl samples and comparable to that for the Pb-Te pair. The combination of increased vacancies and local bond disorder will increase the hole scattering and partially explain the increased resistivity and low $ZT$ value for the 3% sample, in spite of the increase in hole concentration. Thus it is important for understanding the thermoelectric properties to also determine the local structure about dopants that increase the Seebeck coefficient. Possibly doping on sites that have less effect on electron scattering such as the "rattler" site in other systems may prove useful for increasing $ZT$.

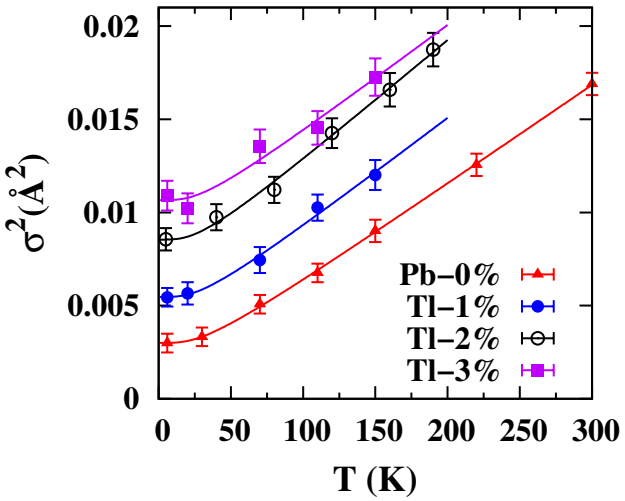


FIG. 7. $\sigma^2$(T) for Tl-Te pair in PbTe:Tl for the three Tl concentrations and for the Pb-Te pair for pure PbTe.The solid lines are fits to a correlated Debye model - see Table I.

## VI. ACKNOWLEDGMENTS

The XAS work was supported under NSF grant DMR1005568. The experiments were performed at SSRL, operated by the DOE, Division of Chemical Sciences. Work at Oak Ridge was supported by the U.S. Department of Energy, Basic Energy Sciences, Materials Sciences and Engineering Division.

[1] B. Sales, Int. J. Appl. Ceram. Tec. **4**, 291 (2007).

[2] Report on basic research needs for solar energy utilization (2005), available at http://www.er.doe.gov/bes/reports/list.html.

[3] A. J. Minnich, M. S. Dresselhaus, Z. F. Ren, and G. Chen, Energy Environ. Sci. **2**, 466 (2009).

[4] J. P. Heremans, V. Jovovic, E. S. Toberer, A. Saramat, K. Kurosaki, A. Charoenphakdee, S. Yamanaka, and G. J. Snyder, Science **321**, 554 (2008).

[5] B. Yu, Q. Zhang, H. Wang, X. Wang, H. Wang, D. Wang, H. Wang, G. J. Snyder, G. Chen, and Z. F. Ren, J. Appl. Phys. **108**, 016104 (2010).

[6] M. Matusiak, E. M. Tunnicliffe, J. R. Cooper, Y. Matsushita, and I. R. Fisher, Phys. Rev. B **80**, 220403 (2009).

[7] Y. Pei, A. LaLonde, S. Iwanaga, and G. J. Snyder, Energy and Environ. Sci. **4**, 2085 (2011).

[8] R. Saravanan and M. C. Robert, J. Phys. Chem. of Solids **70**, 159 (2009).

[9] E. S. Bozin, C. D. Malliakas, P. Souvazis, T. Proffen, N. A. Spaldin, M. G. Kanatzdis, and S. J. Billinge, Science **330**, 1660 (2010).

[10] D. J. Singh, Phys. Rev. B **81**, 195217 (2010).

[11] F. Bridges, T. Keiber, S. Medling, and B. C. Sales, Phys. Status Solidi C **10**, 236 (2013), dOI10.1002/pssc.201200478.

[12] O. Delaire, J. Ma, K. Marty, A. F. May, M. A. McGuire, M. H. Du, D. J. Singh, A. Podlesnyak, G. Ehlers, M. D. Lurnsden, et al., Nat. Materials **10**, 614 (2011).

[13] A. S. Pashinkin, M. S. Mikhailova, A. S. Malkova, and V. A. Fedorov, Inorg. Mat. **45**, 1226 (2009).

[14] A. F. May, M. A. McGuire, J. Ma, O. Delaire, A. Huq, D. J. Singh, W. Cai, and H. Wang, Phys. Rev. B **85**, 035202 (2012).

[15] B. C. Sales, A. F. May, M. A. McGuire, M. B. Stone, D. J. Singh, and D. Mandrus, Phys. Rev. B **86**, 235136 (2012).

[16] T. Keiber, F. Bridges, R. E. Baumbach, and M. B. Maple, Phys. Rev. B **86**, 174106 (2012).

[17] C. H. Booth, R-Space X-ray Absorption Package, 2010 (2010), http://lise.lbl.gov/RSXAP/.

[18] S. Medling and F. Bridges, J. Synch. Rad. **18**, 679 (2011).

[19] P. G. Rustamov, M. A. Alidzhanov, and C. I. Abilov, Phys. Stat. Sol. **12**, 103 (1972).

[20] A. L. Ankudinov, B. Ravel, J. J. Rehr, and S. D. Conradson, Phys. Rev. B **58**, 7565 (1998).

[21] L. Downward, C. H. Booth, W. W. Lukens, and F. Bridges, AIP Conference Proceedings **882**, 129 (2007).

[22] D. Cao, F. Bridges, P. Chesler, S. Bushart, E. D. Bauer, and M. B. Maple, Phys. Rev. B **70**, 094109 (2004).

[23] S. D. Waddington and A. D. C. Grassie, J. Phys. C: Solid State Phys. **21**, 2695 (1988).